

# UC Berkeley

## UC Berkeley Previously Published Works

### Title

Low voltage AC electroluminescence in silicon MOS capacitors

### Permalink

<https://escholarship.org/uc/item/4kr2s8tf>

### Journal

Applied Physics Letters, 121(19)

### ISSN

0003-6951

### Authors

Rahman, IKM Reaz

Uddin, Shiekh Zia

Kim, Hyungjin

et al.

### Publication Date

2022-11-07






### DOI

10.1063/5.0120507

Peer reviewed

RESEARCH ARTICLE | NOVEMBER 08 2022

# Low voltage AC electroluminescence in silicon MOS capacitors

I. K. M. Reaz Rahman ; Shiekh Zia Uddin ; Hyungjin Kim; Naoki Higashitarumizu ; Ali Javey  



*Appl. Phys. Lett.* 121, 193502 (2022)

<https://doi.org/10.1063/5.0120507>

 CHORUS



CrossMark



Applied Physics Letters

Special Topic:  
Advances in Quantum Metrology

Submit Today

# Low voltage AC electroluminescence in silicon MOS capacitors

Cite as: Appl. Phys. Lett. **121**, 193502 (2022); doi: [10.1063/5.0120507](https://doi.org/10.1063/5.0120507)

Submitted: 12 August 2022 · Accepted: 17 October 2022 ·

Published Online: 8 November 2022



View Online



Export Citation



CrossMark

I. K. M. Reaz Rahman,<sup>1,2</sup>  Shiekh Zia Uddin,<sup>1,2</sup>  Hyungjin Kim,<sup>1,2,a)</sup>  Naoki Higashitarumizu,<sup>1,2</sup>   
and Ali Javey<sup>1,2,b)</sup> 

## AFFILIATIONS

<sup>1</sup>Electrical Engineering and Computer Sciences, University of California, Berkeley, California 94720, USA

<sup>2</sup>Materials Sciences Division, Lawrence Berkeley National Laboratory, Berkeley, California 94720, USA

<sup>a)</sup>Present address: Department of Materials Science and Engineering, Yonsei University, Seoul 120-749, Republic of Korea.

<sup>b)</sup>Author to whom correspondence should be addressed: [ajavey@berkeley.edu](mailto:ajavey@berkeley.edu)

## ABSTRACT

Low power silicon based light source and detector are attractive for on-chip photonic circuits given their ease of process integration. However, conventional silicon light emitting diodes emit photons with energies near the band edge where the corresponding silicon photodetectors lack responsivity. On the other hand, previously reported hot carrier electroluminescent silicon devices utilizing a reverse biased diode require high operating voltages. Here, we investigate hot carrier electroluminescence in silicon metal-oxide-semiconductor capacitors operating under transient voltage conditions. During each voltage transient, large energy band bending is created at the edge of the source contact, much larger than what is achievable at a steady state. As a result, electrons and holes are injected efficiently from a single source contact into the silicon channel at the corresponding voltage transient, where they subsequently undergo impact ionization and phonon-assisted interband recombination. Notably, we show low voltage operation down to 2.8 V by using a 20 nm thick high- $\kappa$  gate dielectric. We show further voltage scaling is possible by reducing the gate dielectric thickness, thus presenting a low voltage platform for silicon optoelectronic integrated circuits.

Published under an exclusive license by AIP Publishing. <https://doi.org/10.1063/5.0120507>

In the complementary metal-oxide-semiconductor (CMOS) technology, silicon has lucrative properties: ease of microfabrication,<sup>1,2</sup> prospect for quantum electronics in spin application,<sup>3</sup> and its potential for heterogeneous integration in photonic circuits and optoelectronics.<sup>4</sup> Si CMOS compatibility largely accounts for its success in the avenue of microelectronics, with numerous efforts toward the realization of monolithic integration in electronic and optoelectronic on-chip circuits.<sup>5-7</sup> Silicon already dominates at telecommunication wavelength as waveguides due to low dispersion loss. With a growing need for high-speed communication in signal processing and cloud computing, an all-silicon solution is much desired, where both the light source and detector are fabricated on the same platform. While silicon light emitting diodes (LEDs) demonstrate high quantum efficiencies at infrared wavelength due to their indirect bandgap nature,<sup>8,9</sup> the corresponding photodetectors are insensitive in that regime. For visible emission, silicon falls behind its counterpart, the III-V direct bandgap semiconductors, as a homogenous light source. This shortcoming is partly circumvented by heterogeneous integration of III-Vs on a silicon wafer, which has its complication of lattice mismatch. Thus, visible

electroluminescence (EL) from silicon has attracted intense interest for quite some time, to achieve an overlap of emission wavelength and photodetector responsivity.

Si EL devices have successfully been demonstrated since the early 1960s.<sup>10,11</sup> Most of these initial device structures were  $p-n$  junction diodes,<sup>12-18</sup> operating in forward injection mode or reverse-biased avalanche breakdown regime. Other efforts to extract EL from silicon include but are not limited to anodized porous silicon,<sup>19-25</sup> amorphous silicon,<sup>26</sup> silicon nanocrystals,<sup>27</sup> and silicon-rich oxide<sup>28,29</sup> in the form of reverse-biased  $pn$  junctions or field effect transistors.<sup>15,30</sup> Most of the silicon broadband EL observed with dc excitation is usually divided into three segments: below bandgap, near band edge, and above the bandgap. Hot-carrier bremsstrahlung and intra-band processes seem to account for the former two categories,<sup>13,31</sup> whereas the latter is attributed to the impact ionization of “hot-carriers” followed by interband recombination.<sup>14,15</sup> The very few reports in the literature regarding alternating current EL (ACEL) of silicon fail to reconcile the dominating mechanism of the observed spectra.<sup>22,23,25,27</sup> Since the emission from reverse-biased avalanche breakdown is effectively

the same as pulsed excitation, the purpose of this work is to revisit the concept of silicon EL with ac voltage in a metal–oxide–semiconductor (MOS) structure, to gain a fundamental understanding of the ACEL in indirect bandgap material, thereby advancing the interest of silicon as a homogenous on-chip light source for optoelectronic integrated circuits (OEICs).

A back-gated silicon-on-insulator (SOI) is used in a MOS capacitor structure (see the [supplementary material](#)) to investigate luminescence in silicon with a square wave pulse. For the source contact, nickel is chosen for its favorable Schottky barrier height to electrons over holes when formed into metal–silicide contact by annealing.<sup>32</sup> [Figures 1\(a\)](#) and [1\(b\)](#) show the schematic of the device structure together with the optical micrograph. From the EL image [[Fig. 1\(c\)](#)], we confirm that most of the emission takes place within a few micrometers along the periphery of the source contact ([Fig. S1](#)). Light out-coupling from the SOI structure needs to be addressed to account for the spectral shape as will be discussed later in this Letter. The EL spectra from the MOS capacitor are mostly above bandgap [[Fig. 1\(d\)](#)] with a well-defined peak in the 1.5–1.7 eV range, concomitant with the interband recombination process as suggested by previous reports.<sup>14,33</sup> The broadband nature of the EL arises from the phonon-assisted indirect band-to-band recombination, where the primary electron/hole has excess energy more than the indirect bandgap as investigated from reflectance measurement ([Fig. S2](#) of the [supplementary material](#)). Optical phonon emission during thermalization of energetic “hot carriers” competes with impact ionization as we traverse from  $\Gamma$  to X-valley in the silicon bandstructure<sup>34</sup> [[Fig. 2\(a\)](#)]. Nevertheless, the probability for generation of secondary carriers is still high enough even after single phonon emission to conserve momentum. This implies, having lost energy to varying extent, some of the “hot carriers” recombine radiatively at different heights of the conduction band trajectory in the  $E$ - $k$  diagram before they can reach the conduction band minimum near the X-valley.<sup>35</sup> The intra-band emission is unlikely to account for this above-mentioned bandgap EL. Bremsstrahlung, on

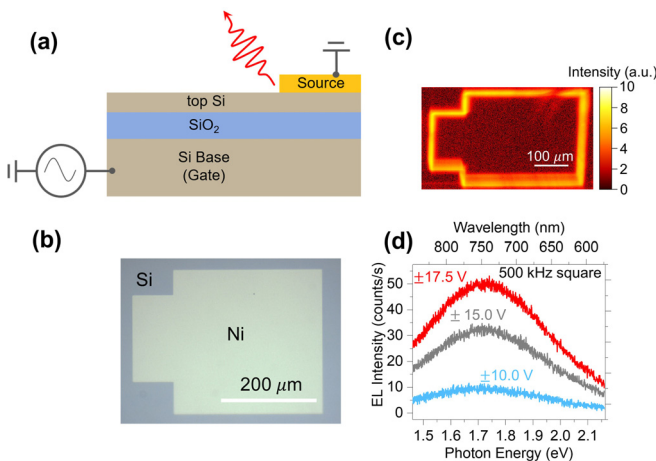


**FIG. 1.** Transient electroluminescence in silicon. (a) Schematic cross section of the device. (b) Optical micrograph. (c) EL image of the device portraying luminescence along the periphery of Schottky junction under ac excitation. (d) EL spectra at various gate voltages for a silicon-on-insulator device having top silicon thickness of 12 nm and buried oxide 25 nm.

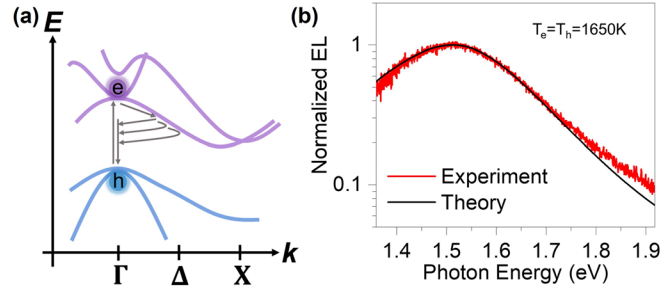


**FIG. 2.** Theoretical spectrum of a silicon MOS capacitor. (a) Schematic illustration of the  $E$ - $k$  diagram showing the phonon-assisted indirect band-to-band recombination of the hot carriers after excited deep into the conduction band. The energetic hot carriers thermalize quickly by emission of optical phonon. Some of these carriers undergo radiative recombination with various energies along the  $\Gamma$  to X trajectory in the  $k$ -space, accounting for the broad EL spectrum. (b) Theoretical spectrum of silicon EL using the hot carrier recombination model. The spectrum matches reasonably well with measured EL data of a representative silicon MOS capacitor with a hot carrier temperature of 1650 K.

the other hand, would support a monotonously increasing spectra with wavelength, which is in stark contrast to our observation. Additionally, as we approach the direct bandgap of silicon, electron–hole pair production should dominate any recombination within the channel, leading to the high energy tail of the EL spectrum above 2 eV.<sup>33</sup>

Bearing the recombination pathway in mind, we can analytically formulate the EL spectra by noting that the emission rate of photons should depend on the photon energy and density of states of electron/hole in the conduction/valence band and the energy distribution of the hot carriers. According to Wolff,<sup>36</sup> the hot electron distribution is proportional to

$$f(E, T_e) \propto \exp\left(-\frac{E}{k_B T_e}\right) \left(1 - \frac{I_i\left(\frac{E}{k_B T_e}\right)}{I_i\left(\frac{E_0}{k_B T_e}\right)}\right), \quad (1)$$

where  $I_i(x) = \int_{-\infty}^x \exp(z)/z dz$  is the exponential integral,  $E$  is the hot electron energy measured from the conduction band edge,  $k_B$  is the Boltzmann constant,  $T_e$  is the hot electron temperature, and  $E_0 \approx 1.5$  eV is the threshold for impact ionization. The hot hole distribution is taken to be quasi-Maxwellian due to the large threshold for ionization,<sup>37,38</sup> approximated as

$$1 - f(h\nu - E_g - E, T_h) \approx \exp\left(-\frac{h\nu - E_g - E}{k_B T_h}\right), \quad (2)$$

where  $h\nu$  is the emission photon energy,  $E_g$  is the indirect bandgap, and  $T_h$  corresponds to hot hole temperature.

The hot carrier recombination model then has the following form:

$$H_c(h\nu) \propto \int_0^{h\nu - E_g} h\nu \cdot D_c(E) \cdot D_h(h\nu - E_g - E) \cdot f(E, T_e) \cdot [1 - f(h\nu - E_g - E, T_h)] dE, \quad (3)$$

where  $D_{e(h)}(x)$  corresponds to density of states of electron (hole) in the conduction (valence) band. It is to be noted that during the voltage transients, the hot carriers undergo a range of temperatures from ambient condition to some thousand Kelvin. Although a proper weighting function for each temperature is more apt to model the dynamics of the square wave pulse, our objective was to obtain a general line shape through use of an average temperature ( $T_e = T_h \approx 1650$  K) that matches experimental data to a reasonable degree [Fig. 2(b)]. The theoretical spectrum also needs to be corrected for light outcoupling, since multiple reflections occur at the oxide–semiconductor and semiconductor–air interface before the EL reaches the detector (Fig. S3 of the supplementary material).

So far, we have discussed the recombination phenomena accounting for the shape of the EL spectrum. To understand the temporal behavior of the charge carriers within the system, we perform 2D numerical simulations<sup>39,40</sup> (see the supplementary material) complemented with time resolved EL (TREL) measurements (Figs. 3 and S4). When a square voltage waveform having amplitude  $\pm V_g$  is applied between the gate-source terminal of the MOS capacitor, there is instantaneous large energy band bending near the metal–semiconductor junction during the voltage level transition, accommodating injection of carriers at either pulse edge [Fig. 3(b)]. This is due to the

capacitive nature of the device which precludes abrupt voltage change in the circuit. Therefore, the entire voltage drop ( $\sim 2V_g$ ) takes place across the most resistive part of the device, the Schottky junction, resulting into a momentary high electric field near the interface to facilitate impact ionization. The measured TREL from the MOS capacitor supports this theory [Fig. 3(c)], where the asymmetry in the integrated EL count at each half-cycle results from the distinct Schottky barrier height to electron-hole. The higher integrated EL count during negative to positive  $V_g$  means that electron injection is more conducive to nickel–silicide Schottky contact, leading to larger current peaks at these respective pulse edges.

As long as the device operates in a high electric field, impact ionization continues to generate energetic “hot-carriers” deep within the conduction band of silicon, the thermalization of which requires picoseconds to nanoseconds.<sup>41</sup> For a voltage pulse width of hundreds of nanoseconds, it suffices to say that the TREL will decay within the first few hundred picoseconds as portrayed in Fig. 3(c). Once the threshold for impact ionization is reached, the EL should scale linearly with frequency as can be seen in Fig. 4(a) until saturation takes over, at which point the overlap of successive ionization events leads to sublinearity. Likewise, through the application of a large gate voltage, a greater electric field should induce more interband recombination at a particular

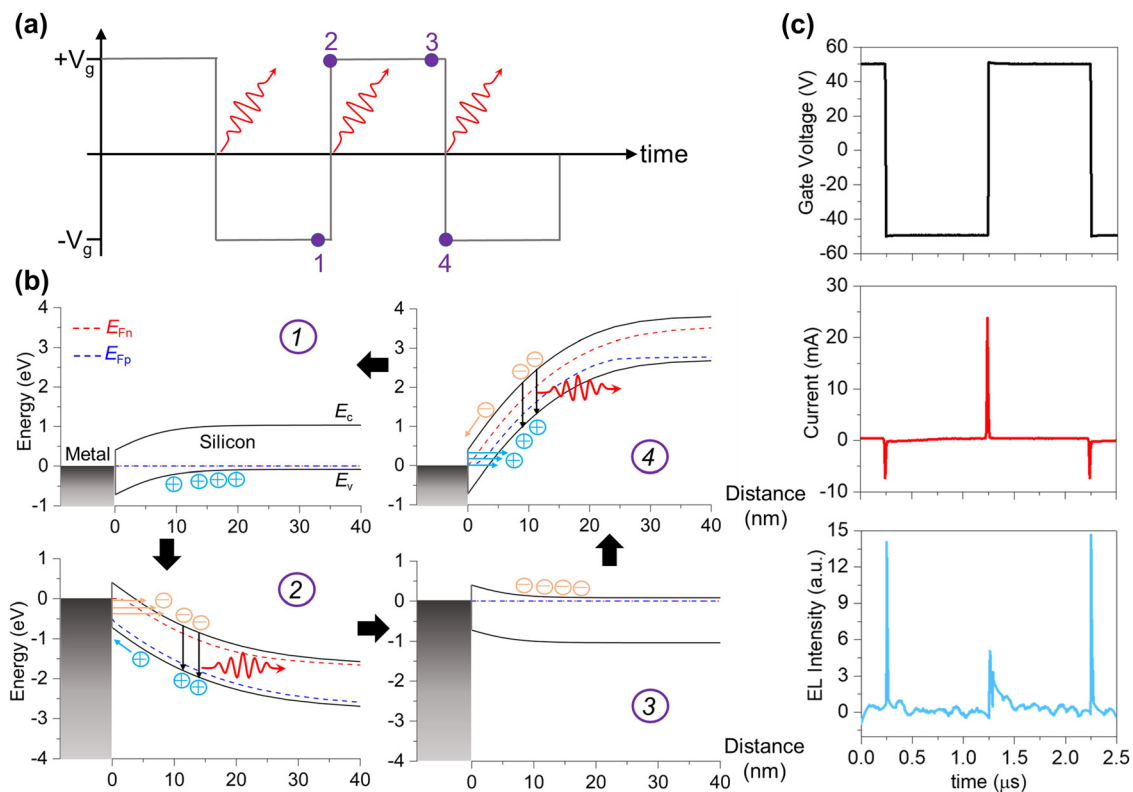


**FIG. 3.** Operating mechanism of an ACEL device. (a) Gate voltage pulse applied to the simulated device. (b) The temporal change in the energy band diagram during one complete cycle of the pulse. The system is in equilibrium at steady-state (instance 1 and 3) having excess holes and electrons, respectively, within the semiconductor. During the voltage level transition (instance 2 and 4), large band bending near the Schottky junction promotes injection of electrons and holes, respectively. The Fermi energy level splitting depicts this scenario at each time-point. (c) TREL of a representative silicon MOS capacitor. The electroluminescence takes place at the sharp transition of the input square wave as anticipated by theory.

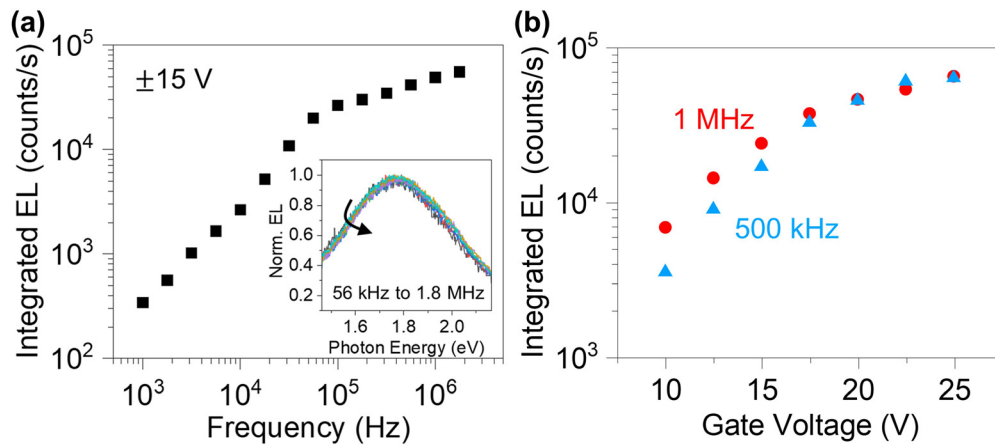


**FIG. 4.** Integrated EL intensity at different voltages and frequencies. (a) EL intensity as a function of frequency, showing a linear dependence of recombination events with frequency until the device reaches sublinearity. The inset shows that there is no shift of the emission peak wavelength with frequency. (b) EL intensity variation with gate voltage at different frequencies. The channel thickness of the device is 12 nm with an underlying 25 nm buried oxide.

frequency [Fig. 4(b)]. Within the range of voltage and frequency applied, there is no degradation of the channel from impact ionization as evident from the overlaid normalized spectra.

It is known that the operating voltage of an ACEL device can be scaled by (i) using a voltage pulse with a shorter transient time and (ii) scaling the gate oxide.<sup>42,43</sup> The former is limited by the instrument switching speed while the latter depends on the quality of the deposited oxide. We deposited a thin layer of  $\text{ZrO}_2$  oxide on SOI to make a top-gate contact device to demonstrate EL emission with a low operating voltage [Fig. 5(a)]. The inset figure reveals that impact ionization starts as low as 2.8 V for a 20 nm high- $\kappa$  gate oxide. To initiate impact ionization, an injected carrier must traverse a minimum distance " $l_{ph}$ " from the metal–semiconductor interface without any collision with phonons, where  $l_{ph}$  is commonly termed as the optical phonon mean free path. Going back to the energy band bending scenario, the onset

of ionization can be defined irrespective of the oxide thickness by a voltage drop ( $\Delta V_{th}$ ) from the metal–semiconductor interface across the phonon mean free path, typically  $\approx 10$  nm in silicon.<sup>44,45</sup> Using the experimental gate voltage for onset of impact ionization in 20 nm  $\text{ZrO}_2$ , we obtained  $\Delta V_{th}$  with numerical simulations (see the supplementary material). We find that a minimum of 410 meV band bending is required above the bandgap to obtain EL in a characteristic silicon MOS capacitor [Fig. 5(b)] as predicted by Wolff.<sup>36</sup> As we scale the oxide thickness down to few nanometers, the same  $\Delta V_{th}$  can be achieved with a much lower operating gate voltage, highlighting its potential for use in OEICs.

In conclusion, we studied the emission mechanism of silicon MOS capacitors with pulsed excitation. The prevalent theory of EL from reverse-biased silicon pn junction juxtaposed with the more complex dynamics of transient simulation helps to clarify the

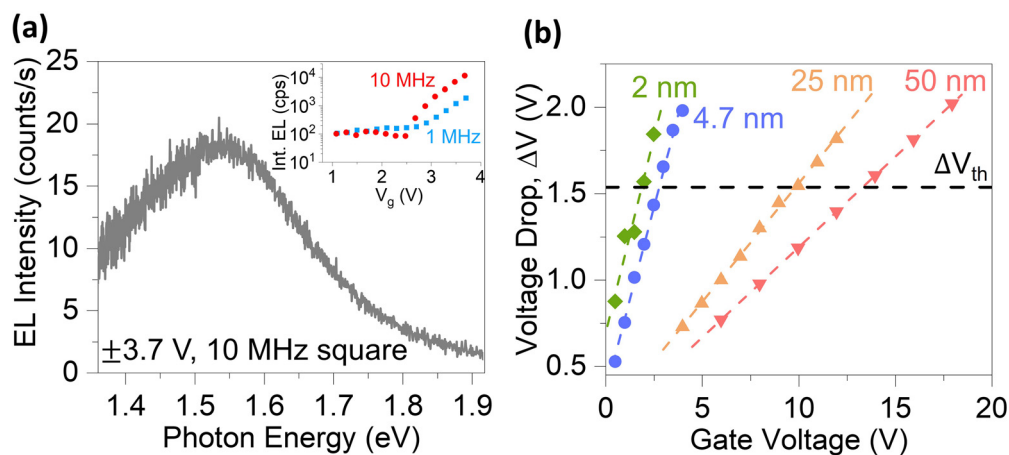


**FIG. 5.** Voltage scaling of ACEL device. (a) EL spectrum of a scaled oxide silicon MOS capacitor having 20 nm  $\text{ZrO}_2$  as the top-gate dielectric. The inset shows that the integrated EL counts increase exponentially once the threshold for impact ionization is reached. (b) Simulated voltage drop ( $\Delta V$ ) of a silicon MOS capacitor with oxide thickness.  $\Delta V$  is the voltage drop from the source contact edge to the optical phonon mean free path. The dashed line represents the minimum voltage drop  $\Delta V_{th}$  required to induce impact ionization in the silicon channel in part (a), corresponding to an equivalent oxide thickness of 4.7 nm.

recombination process under ac voltage. Essentially the physics of the luminescence is the same which can be captured by a simple hot carrier recombination model, but the use of pulsed voltage over dc allows more controlled emission from hot carriers without having to incur degradation in the channel. The low voltage operation of silicon ACEL means that hot carrier effects can be harnessed to overcome the shortcomings of silicon as a homogenous light source that has so long plagued its venture into the realm of optoelectronics.

See the [supplementary material](#) for more information on device fabrication, electrical and optical characterization, numerical simulation, and correction to light coupling.

This work was funded by the U.S. Department of Energy, Office of Science, Office of Basic Energy Sciences, Materials Sciences and Engineering Division under Contract No. DE-AC02-05-CH11231 (EMAT program KC1201). N.H. acknowledges the support from Postdoctoral Fellowships for Research Abroad of the Japan Society for the Promotion of Science.

## AUTHOR DECLARATIONS

### Conflict of Interest

The authors have no conflicts to disclose.

### Author Contributions

**I K M Reaz Rahman:** Conceptualization (equal); Data curation (equal); Formal analysis (equal); Investigation (equal); Methodology (equal); Project administration (equal); Software (equal); Validation (equal); Writing – original draft (equal); Writing – review and editing (equal). **Shiekh Zia Uddin:** Conceptualization (equal); Data curation (supporting); Formal analysis (equal); Investigation (supporting); Methodology (equal); Validation (equal); Writing – review and editing (supporting). **Hyungjin Kim:** Conceptualization (supporting); Data curation (supporting); Investigation (supporting); Methodology (equal); Validation (supporting); Writing – review and editing (supporting). **Naoki Higashitarumizu:** Data curation (supporting); Formal analysis (supporting); Methodology (equal); Validation (equal); Writing – review and editing (supporting). **Ali Javey:** Conceptualization (equal); Formal analysis (equal); Investigation (equal); Methodology (equal); Supervision (equal); Validation (equal); Writing – review and editing (equal).

### DATA AVAILABILITY

The data that support the findings of this study are available from the corresponding author upon reasonable request.

## REFERENCES

- G. E. Moore, *Daedalus* **125**, 55 (1996).
- C. Jung-Kubiak, J. Gill, T. Reck, C. Lee, J. Siles, G. Chattopadhyay, R. Lin, K. Cooper, and I. Mehdi, in *IEEE Silicon Nanoelectronics Workshop* (IEEE, 2012), pp. 1–2.
- F. A. Zwanenburg, A. S. Dzurak, A. Morello, M. Y. Simmons, L. C. L. Hollenberg, G. Klimeck, S. Rogge, S. N. Coppersmith, and M. A. Eriksson, *Rev. Mod. Phys.* **85**, 961 (2013).
- Z. Zhou, B. Yin, and J. Michel, *Light Sci. Appl.* **4**, e358 (2015).
- M. du Plessis, H. Aharoni, and L. W. Snyman, *IEEE J. Sel. Top. Quantum Electron.* **8**, 1412 (2002).
- L. W. Snyman, M. du Plessis, and H. Aharoni, *Jpn. J. Appl. Phys.* **46**, 2474 (2007).
- B. Huang, X. Zhang, W. Wang, Z. Dong, N. Guan, Z. Zhang, and H. Chen, *Opt. Commun.* **284**, 3924 (2011).
- M. A. Green, J. Zhao, A. Wang, P. J. Reece, and M. Gal, *Nature* **412**, 805 (2001).
- T. Trupke, J. Zhao, A. Wang, R. Corkish, and M. A. Green, *Appl. Phys. Lett.* **82**, 2996 (2003).
- R. Newman, *Phys. Rev.* **100**, 700 (1955).
- A. G. Chynoweth and K. G. McKay, *Phys. Rev.* **102**, 369 (1956).
- B. Huang, W. Wang, Z. Dong, Z. Zhang, W. Guo, and H. Chen, in *8th IEEE International Conference on Group IV Photonics* (IEEE, 2011), pp. 296–298.
- A. L. Lacaita, F. Zappa, S. Bigliardi, and M. Manfredi, *IEEE Trans. Electron Devices* **40**, 577 (1993).
- A. T. Obeidat, Z. Kalayjian, and A. G. Andreou, *Appl. Phys. Lett.* **70**, 470 (1997).
- K. Hublitz and S. A. Lyon, *Semicond. Sci. Technol.* **7**, 567 (1992).
- S. Dutta, R. J. E. Hueting, and A.-J. Annema, *J. Appl. Phys.* **118**, 114506 (2015).
- S. Dutta, P. G. Steeneken, V. Agarwal, J. Schmitz, A. J. Annema, and R. J. E. Hueting, *IEEE Trans. Electron Devices* **64**, 1612 (2017).
- J. Shewchun and L. Y. Wei, *Solid State Electron.* **8**, 485 (1965).
- S. Lazarouk, P. Jaguiro, and S. Katsouba, *Appl. Phys. Lett.* **68**, 1646 (1996).
- F. Namavar, H. P. Maruska, and N. M. Kalkhoran, *Appl. Phys. Lett.* **60**, 2514 (1992).
- A. Halimaoui, C. Oules, and G. Bomchil, *Appl. Phys. Lett.* **59**, 304 (1991).
- L. Tsybeskov, S. P. Dutttagupta, and K. D. Hirschman, *Appl. Phys. Lett.* **68**, 2058 (1996).
- A. Richter, P. Steiner, F. Kozlowski, and W. Lang, *IEEE Electron Device Lett.* **12**, 691 (1991).
- L. T. Canham, *Appl. Phys. Lett.* **57**, 1046 (1990).
- P. M. Fauchet, *J. Lumin.* **70**, 294 (1996).
- S. Fujita and N. Sugiyama, *Appl. Phys. Lett.* **74**, 308 (1999).
- R. J. Walters, G. I. Bourianoff, and H. A. Atwater, *Nat. Mater.* **4**, 143 (2005).
- D. J. Dimaria, J. R. Kirtley, and E. J. Pakulis, *J. Appl. Phys.* **56**, 401 (1984).
- L. S. Liao, X. M. Bao, N. S. Li, X. Q. Zheng, and N. ben Min, *Solid State Commun.* **97**, 1039 (1996).
- K. Xu, *Phys. Status Solidi A* **216**, 1800868 (2019).
- J. Bude, N. Sano, and A. Yoshii, *Phys. Rev. B* **45**, 5848 (1992).
- N. Biswas, J. Gurganus, and V. Misra, *Appl. Phys. Lett.* **87**, 171908 (2005).
- J. Kramer, P. Seltz, E. F. Stelgmeler, H. Auderset, and B. Delley, *Sens. Actuators A* **37–38**, 527 (1993).
- S. Kolodinski, J. H. Werner, T. Wittchen, and H. J. Queisser, *Appl. Phys. Lett.* **63**, 2405 (1993).
- C. H. Cho, C. O. Aspetti, J. Park, and R. Agarwal, *Nat. Photonics* **7**(7), 285 (2013).
- P. A. Wolff, *J. Phys. Chem. Solids* **16**, 184 (1960).
- C. W. Liu, S. T. Chang, W. T. Liu, M. J. Chen, and C. F. Lin, *Appl. Phys. Lett.* **77**, 4347 (2000).
- M. Lahbabi, A. Ahaitouf, M. Fliyou, E. Abarkan, J. P. Charles, A. Bath, A. Hoffmann, S. E. Kerns, and D. v. Kerns, *J. Appl. Phys.* **95**, 1822 (2004).
- D.-H. Lien, M. Amani, S. B. Desai, G. Ho Ahn, K. Han, J.-H. He, J. W. Ager Iii, M. C. Wu, and A. Javey, *Nat. Commun.* **9**, 1229 (2018).
- V. Wang, Y. Zhao, and A. Javey, *Adv. Mater.* **33**, 2005635 (2021).
- Y. Zhang, X. Jia, S. Liu, B. Zhang, K. Lin, J. Zhang, and G. Conibeer, *Sol. Energy Mater. Sol. Cells* **225**, 111073 (2021).
- V. Wang and A. Javey, *ACS Nano* **15**, 15210 (2021).
- S. Zia Uddin, N. Higashitarumizu, H. Kim, I. K. M. R. Rahman, and A. Javey, *Nano Lett.* **22**, 5316 (2022).
- W. Maes, K. de Meyer, and R. van Overstraeten, *Solid State Electron.* **33**, 705 (1990).
- D. J. Bartelink, J. L. Moll, and N. I. Meyer, *Phys. Rev.* **130**, 972 (1963).